Transit Timing Variations for AU Microscopii b & c

Justin M. Wittrock[1], Stefan Dreizler[2], Michael Reefe[1], Peter Plavchan[1], Emily A. Gilbert[3, 4, 5, 6, 7], Thomas Barclay[4, 6], Brett M. Morris[8], Brice-Olivier Demory[8], Diana Dragomir[9], Ian J. M. Crossfield[10], James Ingalls[11], Patrick Lowrance[11], Peter Gao[12], Laurel Kaye[13], Songhu Wang[14], Elisabeth R. Newton[15], Eric Gaidos[16], Bryson L. Cale[1], Mohammed El Mufti[1], Kevin I. Collins[1], Stephen R. Kane[17], Angelle Tanner[18], Jonathan Gagné[19, 20], Elisa V. Quintana[6], Laura D. Vega[6, 21], Joshua E. Schlieder[6], Teresa Monsue[6], Leslie Hebb[22], Keivan G. Stassun[21], Veronica Roccatagliata[23], Richard P. Schwarz[24], T. G. Tan[25], Don J. Radford[26], Christopher Stockdale[27]

[1]George Mason University; [2]Georg-August-Universität; [3]University of Chicago; [4]University of Maryland; [5]The Adler Planetarium; [6]NASA Goddard Space Flight Center; [7]GSFC Sellers Exoplanet Environments Collaboration; [8]University of Bern; [9]University of New Mexico; [10]University of Kansas; [11]California Institute of Technology; [12]University of California, Santa Cruz; [13]University of Oxford; [14]Indiana University; [15]Dartmouth College; [16]University of Hawai'i at Mānoa; [17]University of California, Riverside; [18]Mississippi State University; [19]Planétarium Rio Tinto Alcan; [20]Université de Montréal; [21]Vanderbilt University; [22]Hobart and William Smith Colleges; [23]Universitá di Pisa; [24]CV Ventures LLC; [25]Perth Exoplanet Survey Telescope; [26]Brierfield Observatory; [27]Hazelwood Observatory

Abstract

AU Mic is a relatively bright, nearby (9.7 pc), young (22 Myr) M1V pre-main sequence star hosting two transiting exoplanets AU Mic b and c and a spatially-resolved outer dusty debris disk. This research explores the transit timing variations (TTVs) of AU Mic b and c. For AU Mic b, we present three Spitzer/IRAC (4.5 μm) transits (two new), five TESS Cycle 1 and 3 transits, 11 LCO transits, one PEST-0.30m transit, one Brierfield-0.36m transit, and two transit timing measurements from Rossiter-McLaughlin observations; for AU Mic c, we present three TESS Cycle 1 and 3 transits. We use EXOFASTv2 to jointly model the transits and to obtain the midpoint transit times. We then construct an O-C diagram to map the TTVs. We model the TTVs for AU Mic b and c with Exo-Striker to recover constraints on the mass for AU Mic c. We compare the TTV-derived constraints to a recent radial-velocity mass determination. The results demonstrate that the AU Mic planetary system is dynamically interacting producing detectable TTVs, and the implied orbital dynamics may inform future constraints on the formation mechanisms for this young planetary system. However, stellar activity from flares and rotational spot modulation complicate our analysis of this young system. We recommend future TTV observations of AU Mic b and c to further constrain the dynamical masses and to search for additional planets in the system.

Introduction

- The transit timing variations (TTVs) serves as a useful tool for probing stellar systems for additional planets (Holman & Murray 2005; Agol et al. 2005; Mazeh et al. 2013; Becker et al. 2015).
- TTVs can place a limit on a planet's mass if the system is compact or the planets are in orbital resonance (Gillon et al. 2017; Grimm et al. 2018).
- AU Mic (TOI-2221) is a young (22 ± 3 Myr, Mamajek & Bell 2014), nearby (9.7 pc, Bailer-Jones et al. 2018) BY Draconis variable star with spectral type M1V and relative brightness V=8.81.
- AU Mic is an active star, with numerous flares observed at several wavelengths (Gilbert et al. 2021, Butler et al. 1981; Kundu et al. 1987; Cully et al. 1993; Tsikoudi & Kellet 2000).
- AU Mic hosts a debris disc (Kalas et al. 2004) between 50 & 210 au from the star and two planets b (Plavchan et al. 2020) and c (Gilbert et al. 2021) with periods of 8.46 days and 18.86 days, respectively.
- AU Mic is a unique, viable laboratory for studying the stellar activity of a young M dwarf, the planetary formation, the evolution of exoplanet radii as a function of age, orbital architectures of young giant planet systems, characteristics of young exoplanets, and the interplay between planets and disks.
- We examine the transit timing variations (TTVs) of AU Mic using additional observational data.

Methodology

- 23 AU Mic b transits and 3 AU Mic c transits have been included in the analysis.
- We include b's five and c's three TESS midpoint times from Gilbert et al. (2021), one SPIRou midpoint time from Martioli et al. (2020), and one ESPRESSO midpoint time from Palle et al. (2020).
- The three Spitzer transits have been processed as described in Wittrock et al. (2021).
- The LCO SAAO & SSO, Brierfield, and PEST conducted transit follow-ups of AU Mic b as part of TESS Follow-up Observing Program Working Group (TFOP WG; https://tess.mit.edu/followup), and their data became available on ExoFOP-TESS (https://exofop.ipac.caltech.edu/tess; Akeson et al. 2013).
- We utilized the AstroImageJ (Collins et al. 2017) to create a subset table containing only BJD, normalized flux, flux uncertainty, and detrending columns from the ground-based lightcurves.
- Next, we use EXOFASTv2 (Eastman et al. 2019) to perform joint-model of Spitzer and ground-based datasets and extract their midpoint times.
- Afterward, we model the TTVs by incorporating the midpoint times into Exo-Striker (Trifonov 2019). We attempt a 2-planet model with various eccentricities (circular, mild, and high) and a 3-planet circular model.

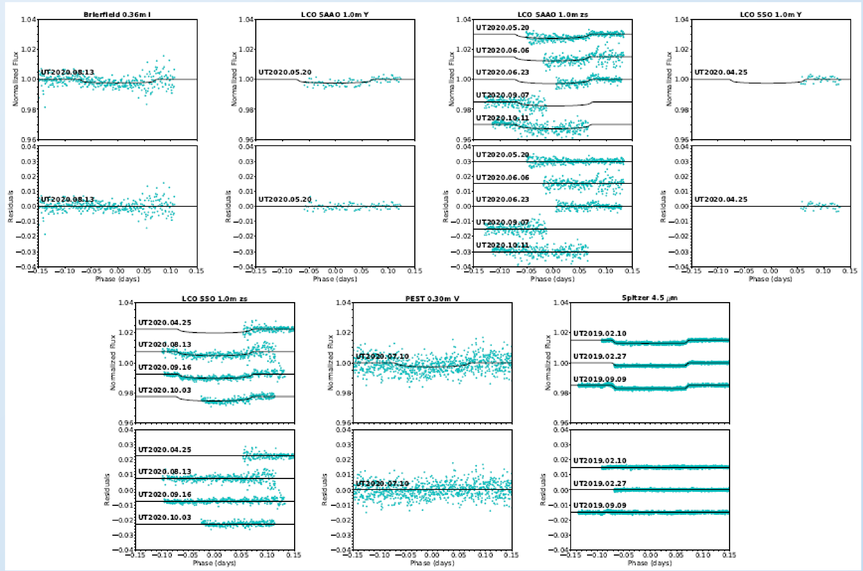

Figure 1: Two-panel plots of comparison between ground-based + Spitzer transits (cyan) and ExoFASTv2's best fit model (black) for AU Mic b. The transit models are in the upper panels, and the residuals are in the lower panels. Brierfield is obtained at transit 88; LCO SAAO at 78, 80, 82, 91, & 95; LCO SSO at 75, 88, 92, & 94; PEST at 84; and Spitzer at 23, 25, & 48, relative to the first TESS transit.

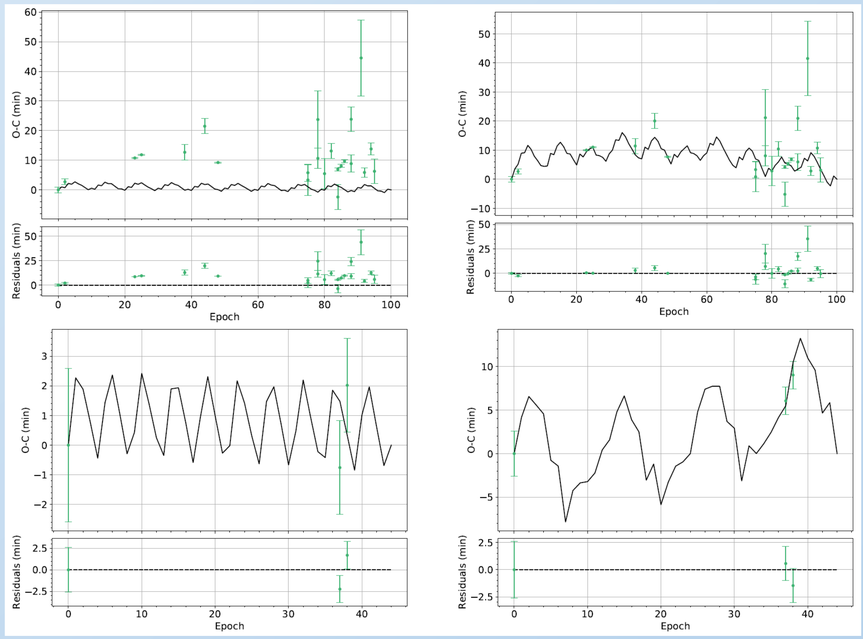

Figure 2: Comparison between TTV data (green) and Exo-Striker's best-fit model (black). The top row is of planet b, and the bottom row is of planet c. The left column is a 2-planet model, and the right column is a 3-planet model. The eccentricities are circular in both cases. An exploration of eccentric 2-planet TTV solutions required high eccentricities inconsistent with the light curve modeling posteriors in ExoFAST and in Plavchan et al. (2020) and Gilbert et al. (2021).

Acknowledgements

Funding for the TESS mission is provided by NASA's Science Mission directorate. This research has made use of the Exoplanet Follow-up Observation Program website, which is operated by the California Institute of Technology, under contract with the National Aeronautics and Space Administration under the Exoplanet Exploration Program. This paper includes data collected by the TESS mission, which are publicly available from the Mikulski Archive for Space Telescopes (MAST).

Discussion

- The O-C diagram from a complementary photodynamical analysis not presented here (Wittrock et al. 2021) indicates that the derived transit times are sensitive to the methods employed for accounting for the stellar activity.
- However, the analysis done by Gilbert et al. (2021) shows no dependence of transit timing on activity after marginalizing over models for the flares and spot modulation. The TESS transit times are fairly constant to within ~4 minutes. Additionally, the Spitzer data have greater photometric precision, are less impacted by stellar activity at 4.5 microns, and show significant deviations from a linear ephemeris than derived by the TESS data alone.
- While our TTV analysis strongly suggests the existence of a third middle non-transiting planet consistent with the candidate period identified in Cale et al. (2021), it is possible that there is some unaccounted-for effect in the derived TTV uncertainties, although we deem this scenario unlikely given the above marginalization over our activity models.
- Additional TTVs are needed to vet the possibility of the RV candidate highlighted in Cale et al. (2021), and to refine our photodynamical analysis, such as would be possible with the Pandora mission, CHEOPS, Ariel, or JWST with multi-band space-photometry.
- Additional ground and space-based observations of b and c transits may confirm or rule out the third planet or the unaccounted-for stellar activity effects.

Table 1: Exo-Striker-generated best-fit and MCMC parameters for a two-planet model in circular case.

Parameter	Best-fit		MCMC	
	Planet b	Planet c	Planet b	Planet c
K [m/s]	11.5318	7.2749	2.0594 ± 2.8155	61.2051 ± 6.7286
P [day]	8.4627	18.8659	8.4606 ± 0.0005	18.8603 ± 0.0017
e	0.0238	0.0000	0.0435 ± 0.0023	0.0190 ± 0.0090
ω [deg]	90.1782	89.8116	101.3512 ± 2.4171	202.3579 ± 25.5393
M_0 [deg]	342.9866	126.8285	330.9529 ± 2.6168	12.2116 ± 25.6967
i [deg]	89.4501	90.4717	88.8813 ± 1.4315	92.3200 ± 1.6105
Ω [deg]	0.0001	0.0003	19.4066 ± 21.6847	32.4073 ± 22.8235

NOTE—$-\ln \mathcal{L} = (12.1361, -804.7715)$ for best-fit and MCMC respectively.

Table 2: Exo-Striker-generated best-fit and MCMC parameters for a three-planet model in circular case.

Parameter	Best-fit			MCMC		
	Planet b	Planet c	Planet d	Planet b	Planet c	Planet d
K [m/s]	10.3746	12.3866	1.6445	19.7845 ± 10.6738	16.1704 ± 3.7952	1.0770 ± 0.2822
P [day]	8.4634	18.8656	12.9211	8.4636 ± 0.0005	18.8701 ± 0.0057	12.9109 ± 0.0151
e	0.0076	0.0000	0.0000	0.0208 ± 0.0107	0.0098 ± 0.0129	0.0020 ± 0.0050
ω [deg]	89.3161	62.1949	0.0000	87.4843 ± 7.2579	66.3204 ± 15.0948	7.0053 ± 13.0391
M_0 [deg]	344.1168	154.4539	100.5487	346.0632 ± 7.5126	151.2287 ± 14.6192	91.5890 ± 14.9975
i [deg]	90.1939	89.0306	78.8998	89.4793 ± 2.6218	89.3865 ± 2.3222	76.5518 ± 4.3387
Ω [deg]	0.0000	0.0000	6.7383	6.2850 ± 10.3589	7.4988 ± 7.6058	12.7344 ± 7.9190

NOTE—$-\ln \mathcal{L} = (93.3561, -1385.3207)$ for best-fit and MCMC respectively.

References

Agol, E., Steffen, J., Sari, R., & Clarkson, W. 2005, MNRAS, 359, 567, doi: 10.1111/j.1365-2966.2005.08922.x
Akeson, R. L., Chen, X., Ciardi, D., et al. 2013, PASP, 125, 989, doi: 10.1086/672273
Bailer-Jones, C. A. L., Rybizki, J., Fouesneau, M., Mantelet, G., & Andrae, R. 2018, AJ, 156, 58, doi: 10.3847/1538-3881/aacb21
Becker, J. C., Vanderburg, A., Adams, F. C., Rappaport, S. A., & Schwengeler, H. M. 2015, ApJL, 812, L18, doi: 10.1088/2041-8205/812/2/L18
Butler, C. J., Byrne, P. B., Andrews, A. D., & Doyle, J. G. 1981, MNRAS, 197, 815, doi: 10.1093/mnras/197.3.815
Cale, B., Reefe, M., Plavchan, P., et al. 2021, submitted
Collins, K. A., Kielkopf, J. F., Stassun, K. G., & Hessman, F. V. 2017, AJ, 153, 77, doi: 10.3847/1538-3881/153/2/77
Cully, S. L., Siegmund, O. H. W., Vedder, P. W., & Vallerga, J. V. 1993, ApJL, 414, L49, doi: 10.1086/186993
Eastman, J. D., Rodriguez, J. E., Agol, E., et al. 2019, arXiv e-prints, arXiv:1907.09480.https://arxiv.org/abs/1907.09480
Gilbert, E. A., Barclay, T., Quintana, E., et al. 2021, submitted
Gillon, M., Triaud, A. H. M. J., Demory, B.-O.,et al. 2017, Nature, 542, 456, doi: 10.1038/nature21360
Grimm, S. L., Demory, B.-O., Gillon, M., et al. 2018, A&A, 613, A68, doi: 10.1051/0004-6361/201732233
Holman, M. J., & Murray, N. W. 2005, Science, 307, 1288, doi: 10.1126/science.1107822
Kalas, P., Liu, M. C., & Matthews, B. C. 2004, Science, 303, 1990, doi: 10.1126/science.1093420
Kundu, M. R., Jackson, P. D., White, S. M., & Melozzi, M. 1987, ApJ, 312, 822, doi: 10.1086/164928
Mamajek, E. E., & Bell, C. P. M. 2014, MNRAS, 445, 2169, doi: 10.1093/mnras/stu1894
Martioli, E., Hébrard, G., Moutou, C., et al. 2020, A&A, 641, L1,doi: 10.1051/0004-6361/202038695
Mazeh, T., Nachmani, G., Holczer, T., et al. 2013, ApJS, 208, 16, doi: 10.1088/0067-0049/208/2/16
Palle, E., Oshagh, M., Casasayas-Barris, N., et al. 2020, A&A, 643, A25, doi: 10.1051/0004-6361/202038583
Plavchan, P., Barclay, T., Gagné, J., et al. 2020, Nature, 582, 497, doi: 10.1038/s41586-020-2400-z
Trifonov, T. 2019, The Exo-Striker: Transit and radial velocity interactive fitting tool for orbital analysis and N-body simulations. http://ascl.net/1906.004
Wittrock, J., Dreizler, S., Reefe, M., et al. 2021, in preparation